

Supporting Information

Tuning Hot Carrier Cooling Dynamics by Dielectric Confinement in Two-Dimensional Hybrid Perovskite Crystals

*Jun Yin,^{1,‡} Partha Maity,^{1,‡} Rounak Naphade,¹ Bin Cheng,² Jr-Hau He,² Osman M.
Bakr,¹ Jean-Luc Brédas,³ and Omar F. Mohammed^{1,*}*

¹ Division of Physical Science and Engineering, King Abdullah University of Science and
Technology, Thuwal 23955-6900, Kingdom of Saudi Arabia

² Computer, Electrical, and Mathematical Sciences and Engineering Division, King
Abdullah University of Science and Technology, Thuwal, 23955-6900, Kingdom of
Saudi Arabia

³ School of Chemistry and Biochemistry, Center for Organic Photonics and Electronics (COPE), Georgia Institute of Technology, Atlanta, Georgia 30332-0400, United States

Corresponding Author

omar.abdelsaboor@kaust.edu.sa

‡ These authors contributed equally to this work.

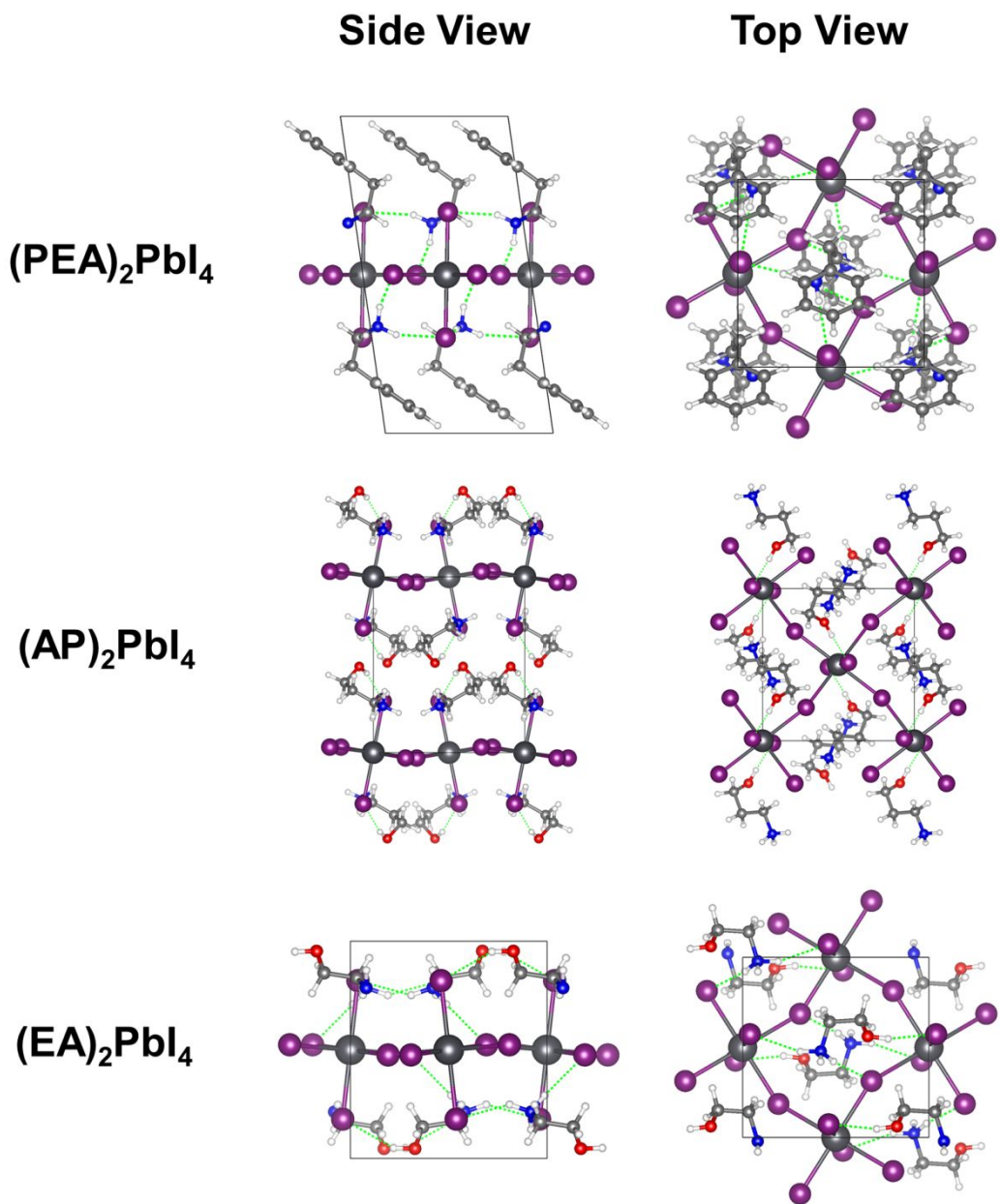


Figure S1. Top and side views of the optimized crystal structures of $(\text{PEA})_2\text{PbI}_4$, $(\text{AP})_2\text{PbI}_4$, and $(\text{EA})_2\text{PbI}_4$. The green dashed lines indicate hydrogen bonding of $\text{N-H}\cdots\text{I}$ or $\text{O-H}\cdots\text{I}$ type.

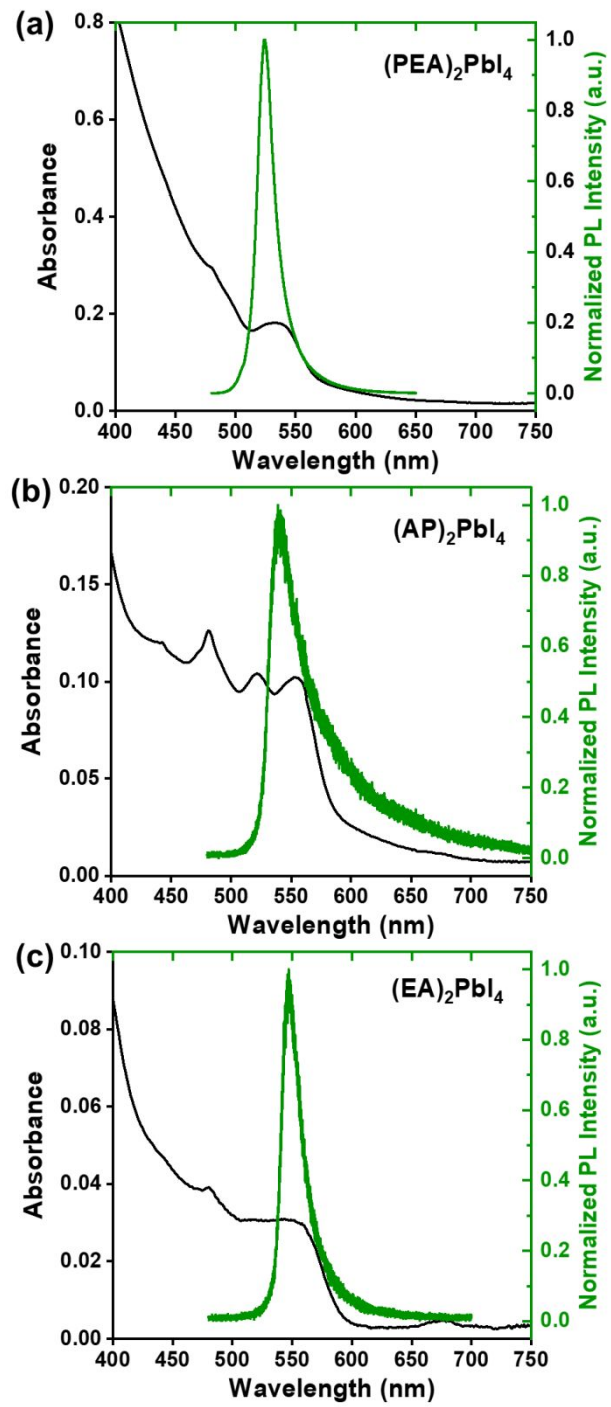


Figure S2. Absorption and normalized photoluminescence spectra of (a) $(\text{PEA})_2\text{PbI}_4$, (b) $(\text{AP})_2\text{PbI}_4$, and (c) $(\text{EA})_2\text{PbI}_4$ single crystals. The absorption spectra were obtained from reflectance spectra measurements (absorbance = $\log(1/\text{reflectance})$).

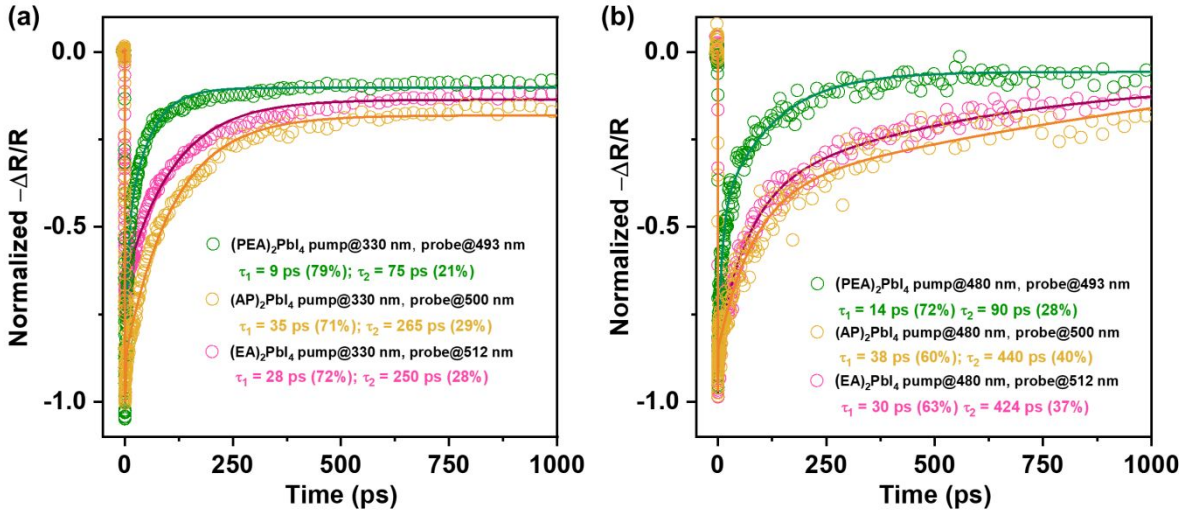


Figure S3. Normalized transient reflectance kinetics of a (PEA)₂PbI₄ crystal probed at 493 nm, a (AP)₂PbI₄ crystal probed at 500 nm, and a (EA)₂PbI₄ crystal probed at 512 nm, using 330 and 480 nm excitations (the solid lines represent fitting of the data with biexponential functions).

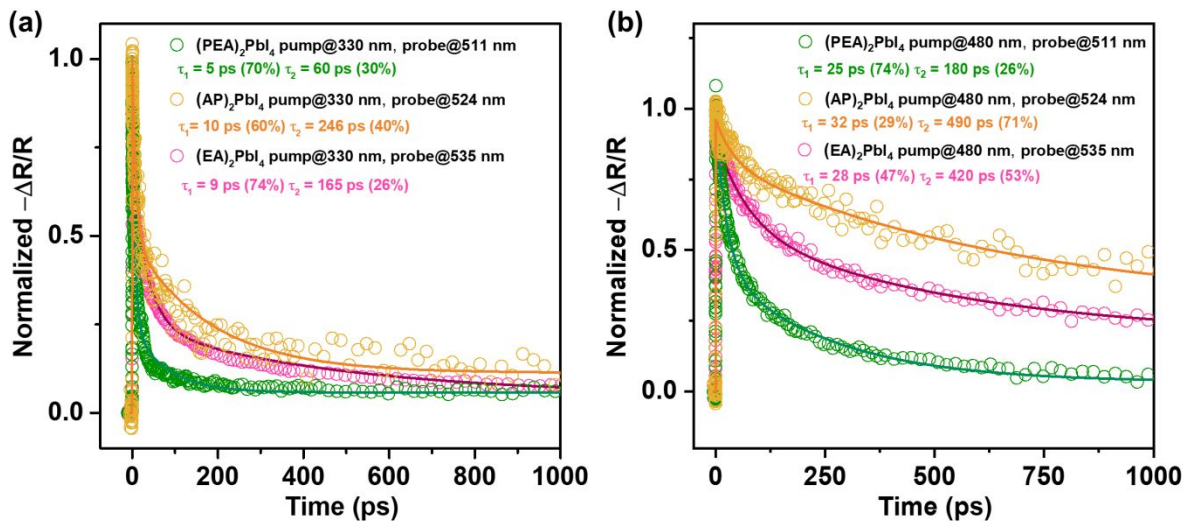


Figure S4. Normalized transient reflectance kinetics of a (PEA)₂PbI₄ crystal probed at 511 nm, a (AP)₂PbI₄ crystal probed at 524 nm, and a (EA)₂PbI₄ crystal probed at 535 nm, using 330 and 480 nm excitations (the solid lines represent fitting of the data with biexponential functions).

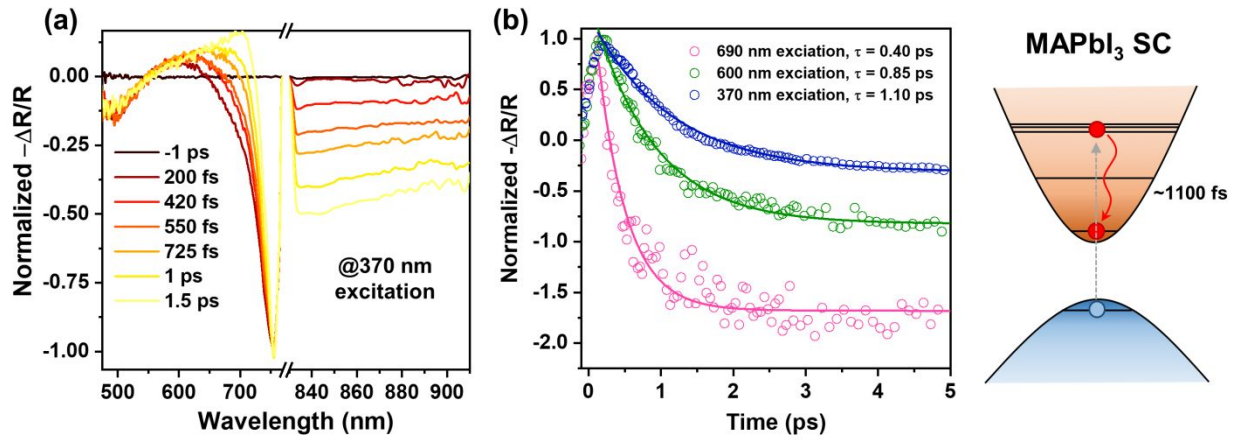


Figure S5. (a) Transient reflectance spectra of the MAPbI₃ single crystal at early delay time (< 2.4 ps) with excitation wavelength of 370 nm; (b) normalized transient reflectance kinetics of MAPbI₃ single crystal probed at 725 nm with 370, 600, and 690 nm excitations (the solid lines represent fitting of the data with an exponential function).

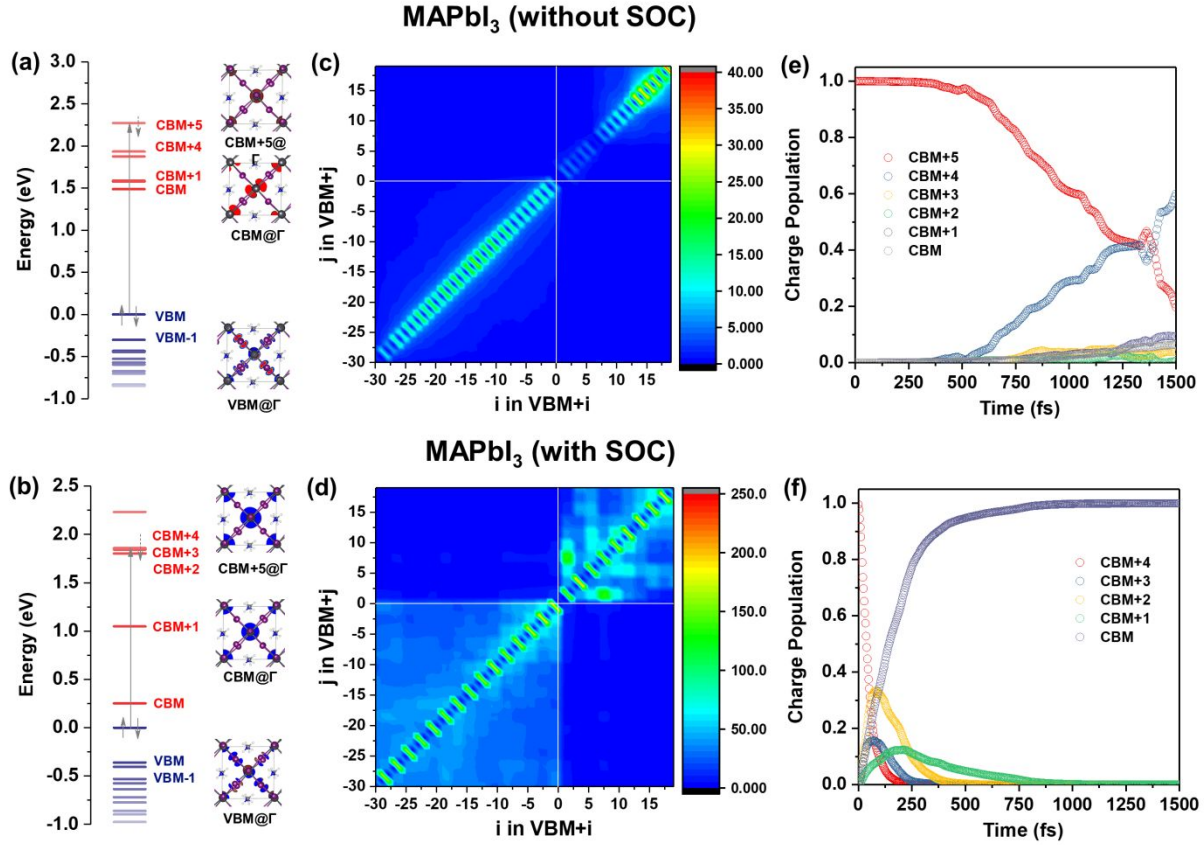


Figure S6. (a, b) Calculated energy levels at the high-symmetry Γ -point of MAPbI₃ together with their electronic charge densities (VBM is set at zero energy); (c, d) average nonadiabatic couplings between the MAPbI₃ orbitals without and with SOC; (e, f) time evolution of hot-electron relaxation starting from CBM+2 for (EA)₂PbI₄ without and with SOC.

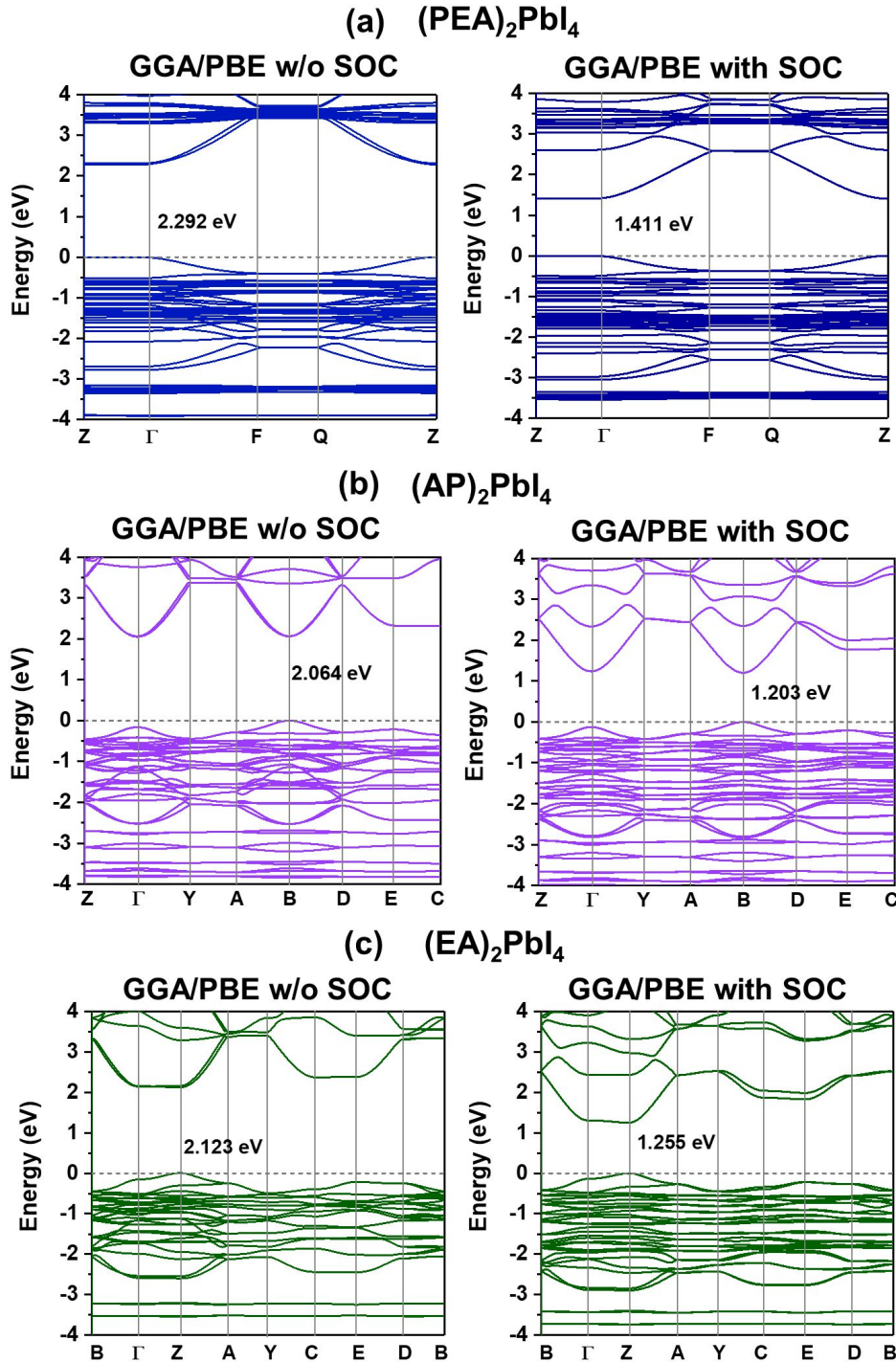


Figure S7. Electronic band structures of (a) $(\text{PEA})_2\text{PbI}_4$, (b) $(\text{AP})_2\text{PbI}_4$, and (c) $(\text{EA})_2\text{PbI}_4$, calculated at the GGA/PBE level of theory without and with spin-orbit coupling (SOC).

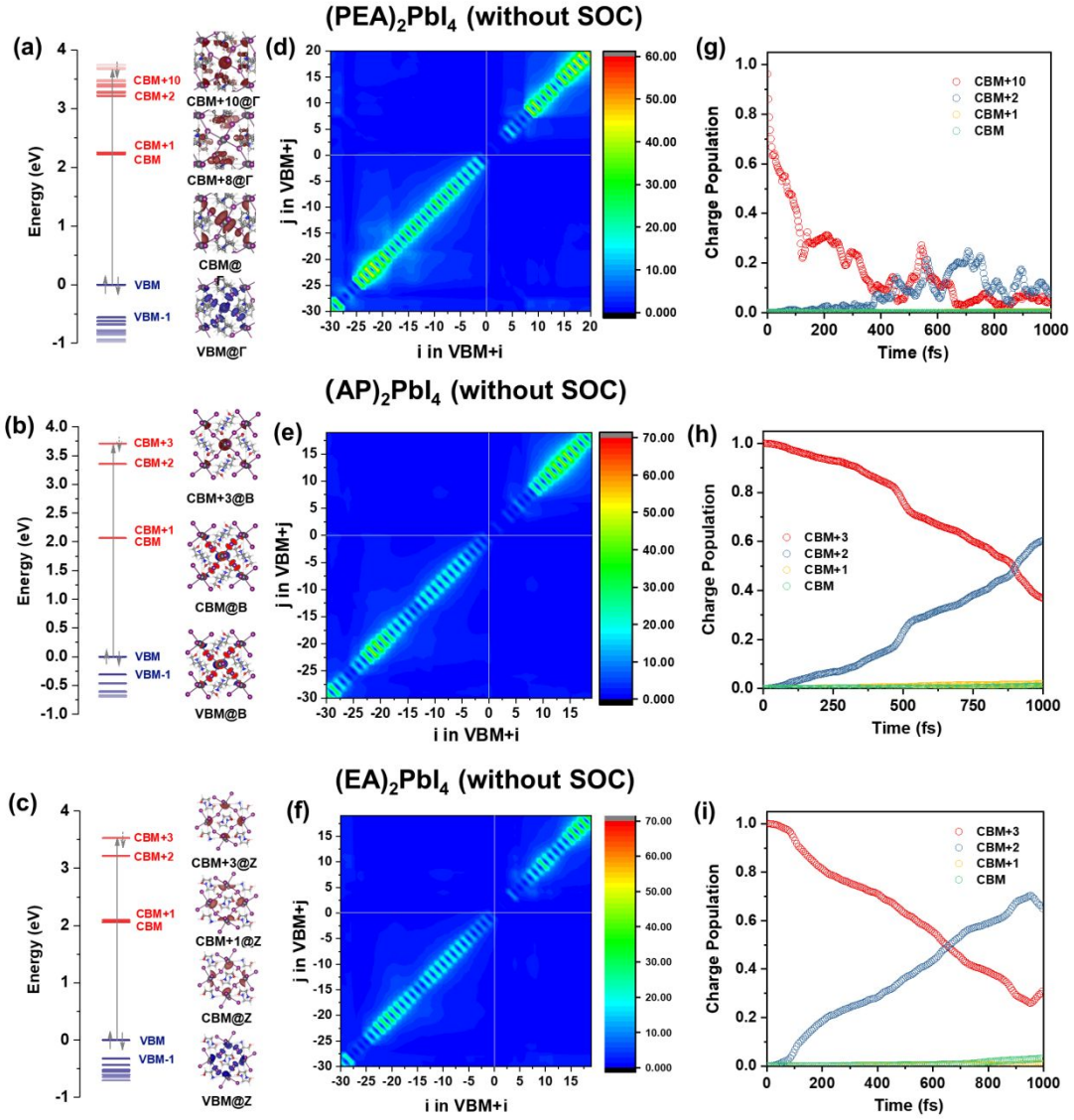


Figure S8. (a, b, c) Calculated orbital levels at the high-symmetry Γ -point of $(\text{PEA})_2\text{PbI}_4$, B-point of $(\text{AP})_2\text{PbI}_4$, and Z-point of $(\text{EA})_2\text{PbI}_4$ together with their electronic charge densities (VBM is set at zero energy); (d, e, f) average nonadiabatic couplings between orbitals of $(\text{PEA})_2\text{PbI}_4$, $(\text{AP})_2\text{PbI}_4$, and $(\text{EA})_2\text{PbI}_4$; (g, h, i) time evolution of hot-electron relaxation starting from CBM+8 (1.47 eV above CBM) for $(\text{PEA})_2\text{PbI}_4$, CBM+3 (1.64 eV above CBM) for $(\text{AP})_2\text{PbI}_4$, and CBM+3 (1.47 eV above CBM) for $(\text{EA})_2\text{PbI}_4$. All the calculations were performed at the GGA/PBE level without SOC.

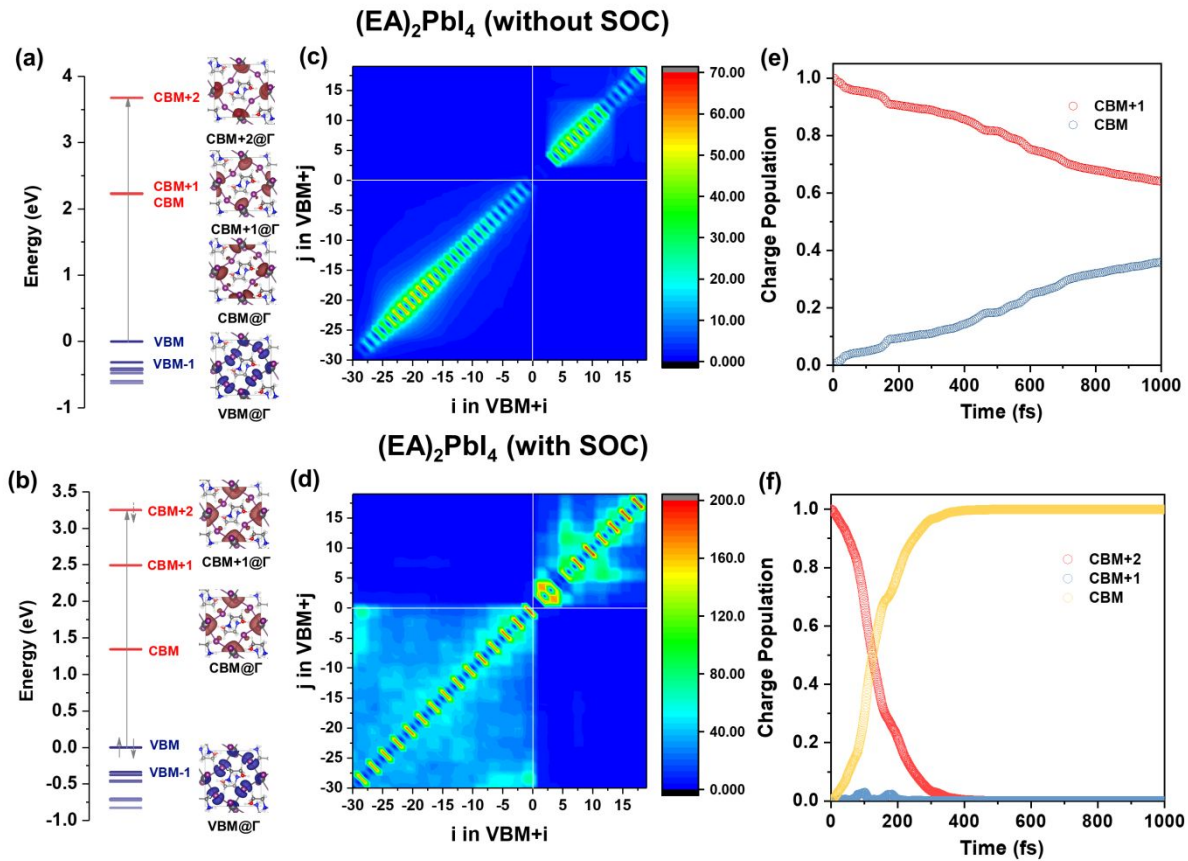


Figure S9. (a, b) Calculated energy levels at the high-symmetry Γ -point of $(EA)_2\text{PbI}_4$ together with their electronic charge densities (VBM is set at zero energy); (c, d) average nonadiabatic couplings between $(EA)_2\text{PbI}_4$ orbitals without and with SOC; (e, f) time evolution of hot-electron relaxation starting from CBM+2 for $(EA)_2\text{PbI}_4$ without and with SOC.

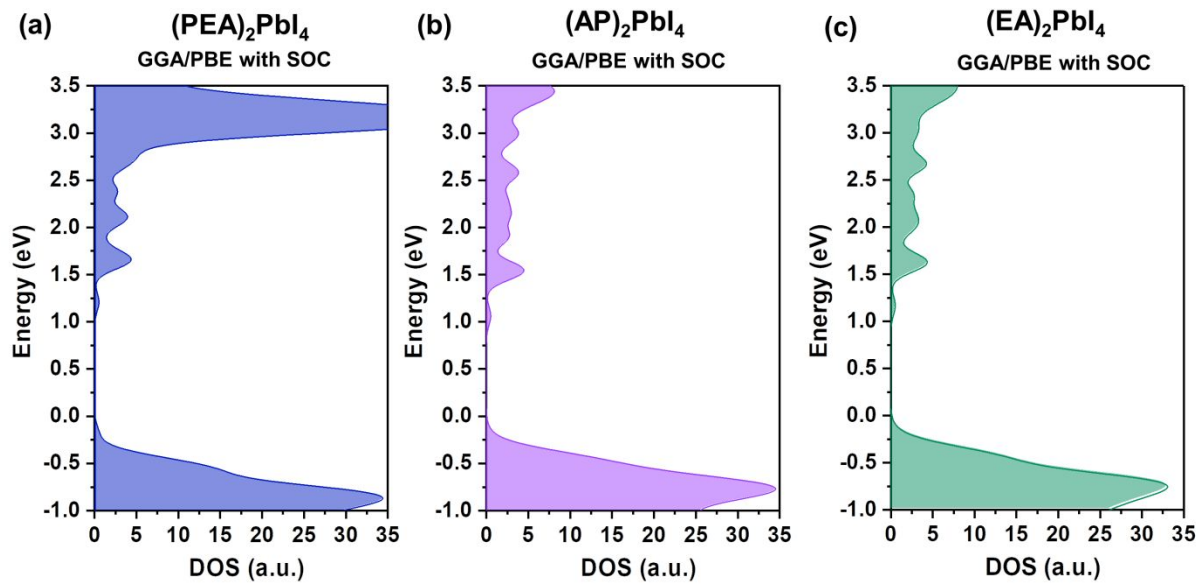


Figure S10. Total density of states (DOS) of (a) $(\text{PEA})_2\text{PbI}_4$, (b) $(\text{AP})_2\text{PbI}_4$, and (c) $(\text{EA})_2\text{PbI}_4$, calculated at the GGA/PBE level of theory with account of SOC.

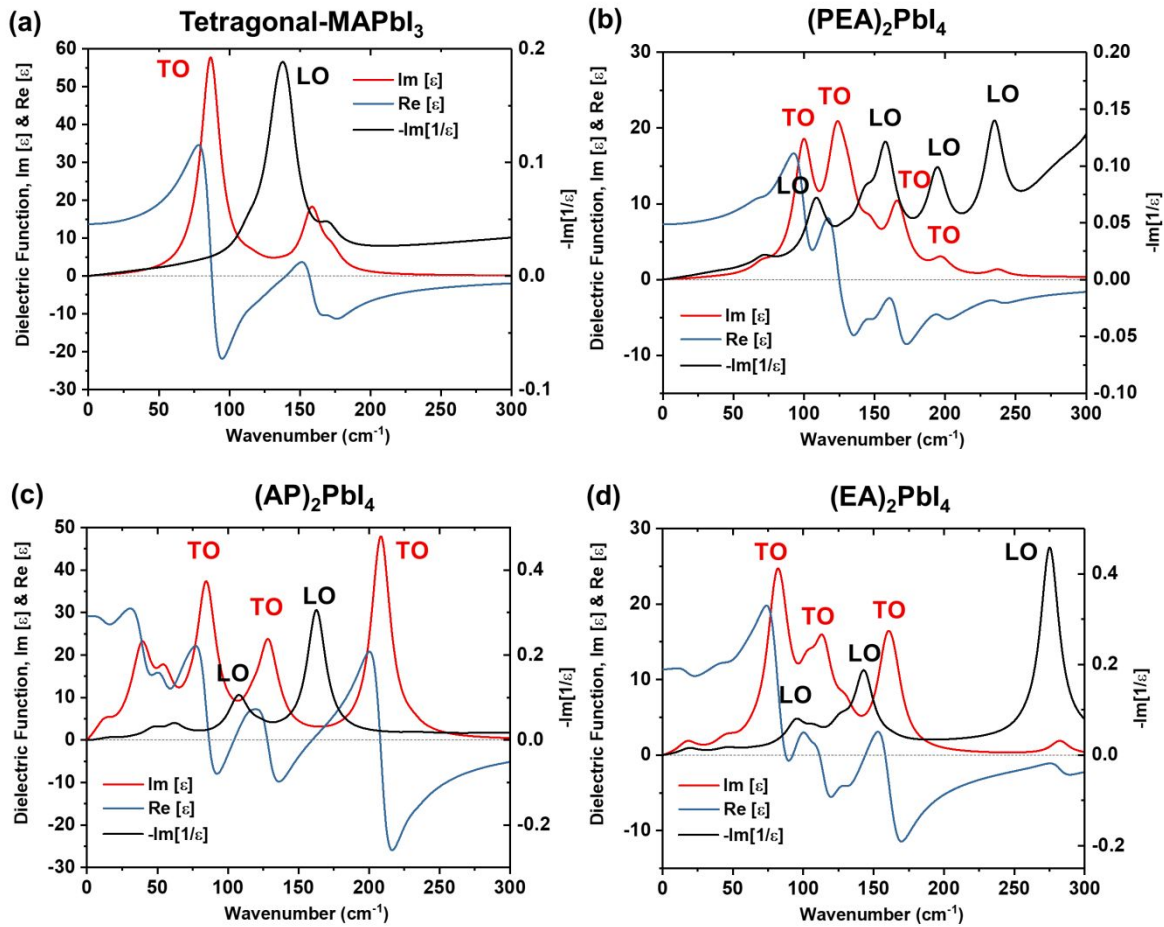


Figure S11. Calculated real part (in blue) and imaginary part (in red) of the dielectric function, and imaginary part of the inverse dielectric function (in black) for (a) tetragonal-phase MAPbI₃, (b) (PEA)₂PbI₄, (c) (AP)₂PbI₄, and (d) (EA)₂PbI₄.

Table S1. Crystallographic and refinement parameters of $(EA)_2PbI_4$.

Empirical formula	C2 H8 I2 N O Pb0.50		
Formula weight	419.49		
Temperature	100(2) K		
Wavelength	0.71073 Å		
Crystal system	Monoclinic		
Space group	P 21/c		
Unit cell dimensions	$a = 10.2263(9)$ Å	$\alpha = 90^\circ$.	
	$b = 9.0447(7)$ Å	$\beta = 100.273(4)^\circ$.	
	$c = 8.9390(8)$ Å	$\gamma = 90^\circ$.	
Volume	813.55(12) Å ³		
Z	4		
Density (calculated)	3.425 Mg/m ³		
Absorption coefficient	17.941 mm ⁻¹		
F(000)	728		
Crystal size	0.30 x 0.20 x 0.15 mm ³		
Theta range for data collection	2.024 to 26.422°.		
Index ranges	-12 <= h <= 12, -11 <= k <= 9, -11 <= l <= 11		
Reflections collected	5886		
Independent reflections	1658 [R(int) = 0.0343]		
Completeness to theta = 25.242°	99.9 %		
Absorption correction	Semi-empirical from equivalents		
Max. and min. transmission	0.9485 and 0.2950		
Refinement method	Full-matrix least-squares on F ²		
Data / restraints / parameters	1658 / 0 / 63		
Goodness-of-fit on F ²	1.084		
Final R indices [I>2sigma(I)]	R1 = 0.0276, wR2 = 0.0676		
R indices (all data)	R1 = 0.0296, wR2 = 0.0687		
Extinction coefficient	n/a		
Largest diff. peak and hole	2.500 and -2.037 e.Å ⁻³		

Table S2. Atomic coordinates ($\times 10^4$) and equivalent isotropic displacement parameters ($\text{\AA}^2 \times 10^3$) for $(\text{EA})_2\text{PbI}_4$. U(eq) is defined as one third of the trace of the orthogonalized U^{ij} tensor.

	x	y	z	U(eq)
Pb(1)	5000	10000	5000	25(1)
I(1)	1862(1)	9568(1)	4308(1)	34(1)
I(2)	5201(1)	7910(1)	7956(1)	42(1)
C(1)	1733(8)	5249(9)	3669(8)	45(2)
C(2)	1484(7)	3643(9)	3599(8)	45(2)
N(1)	2201(6)	5730(7)	5270(6)	43(1)
O(1)	518(5)	3311(6)	4478(6)	48(1)

Table S3. Experimental bond lengths (\AA) and angles ($^\circ$) for $(\text{EA})_2\text{PbI}_4$.

Bond Length (\AA)		Bond Angle ($^\circ$)	
Pb(1)-I(1)	3.1815(5)	I(1)-Pb(1)-I(1)#1	180
Pb(1)-I(1)#1	3.1815(5)	I(1)-Pb(1)-I(2)	90.120(11)
Pb(1)-I(2)	3.2257(4)	I(1)#1-Pb(1)-I(2)	89.880(11)
Pb(1)-I(2)#1	3.2258(4)	I(1)-Pb(1)-I(2)#1	89.880(11)
Pb(1)-I(2)#2	3.2313(4)	I(1)#1-Pb(1)-I(2)#1	90.120(12)
Pb(1)-I(2)#3	3.2313(4)	I(2)-Pb(1)-I(2)#1	180
I(2)-Pb(1)#4	3.2314(4)	I(1)-Pb(1)-I(2)#2	87.346(11)
C(1)-C(2)	1.475(10)	I(1)#1-Pb(1)-I(2)#2	92.654(11)
C(1)-N(1)	1.490(9)	I(2)-Pb(1)-I(2)#2	89.120(7)
C(1)-H(1A)	0.99	I(2)#1-Pb(1)-I(2)#2	90.880(8)
C(1)-H(1B)	0.99	I(1)-Pb(1)-I(2)#3	92.654(11)
C(2)-O(1)	1.400(8)	I(1)#1-Pb(1)-I(2)#3	87.346(11)
C(2)-H(2A)	0.99	I(2)-Pb(1)-I(2)#3	90.880(7)
C(2)-H(2B)	0.99	I(2)#1-Pb(1)-I(2)#3	89.120(8)
N(1)-H(1C)	0.91	I(2)#2-Pb(1)-I(2)#3	180
N(1)-H(1D)	0.91	Pb(1)-I(2)-Pb(1)#4	159.929(18)
N(1)-H(1E)	0.91	C(2)-C(1)-N(1)	110.6(6)
O(1)-H(1)	0.84	C(2)-C(1)-H(1A)	109.5
		N(1)-C(1)-H(1A)	109.5
		C(2)-C(1)-H(1B)	109.5
		N(1)-C(1)-H(1B)	109.5
		H(1A)-C(1)-H(1B)	108.1
		O(1)-C(2)-C(1)	108.8(6)
		O(1)-C(2)-H(2A)	109.9
		C(1)-C(2)-H(2A)	109.9
		O(1)-C(2)-H(2B)	109.9
		C(1)-C(2)-H(2B)	109.9
		H(2A)-C(2)-H(2B)	108.3
		C(1)-N(1)-H(1C)	109.5
		C(1)-N(1)-H(1D)	109.5
		H(1C)-N(1)-H(1D)	109.5
		C(1)-N(1)-H(1E)	109.5

H(1C)-N(1)-H(1E)	109.5
H(1D)-N(1)-H(1E)	109.5
C(2)-O(1)-H(1)	109.5

Symmetry transformations used to generate equivalent atoms:

#1 -x+1,-y+2,-z+1 #2 x,-y+3/2,z-1/2 #3 -x+1,y+1/2,-z+3/2
#4 -x+1,y-1/2,-z+3/2

Table S4. Crystallographic and refinement parameters of (PEA)₂PbI₄.

Empirical formula	C16 H24 I4 N2 Pb	
Formula weight	959.16	
Temperature	100(2) K	
Wavelength	0.71073 Å	
Crystal system	Triclinic	
Space group	P -1	
Unit cell dimensions	a = 8.6879(4) Å b = 8.6903(5) Å c = 16.4242(8) Å	α= 94.496(2)°. β= 100.523(2)°. γ = 90.568(2)°.
Volume	1215.06(11) Å ³	
Z	2	
Density (calculated)	2.622 Mg/m ³	
Absorption coefficient	12.025 mm ⁻¹	
F(000)	856	
Crystal size	0.10 x 0.08 x 0.02 mm ³	
Theta range for data collection	1.265 to 26.419°.	
Index ranges	-10<=h<=8, -10<=k<=10, -20<=l<=20	
Reflections collected	20297	
Independent reflections	4987 [R(int) = 0.0354]	
Completeness to theta = 25.000°	99.9 %	
Absorption correction	Semi-empirical from equivalents	
Max. and min. transmission	0.80 and 0.43	
Refinement method	Full-matrix least-squares on F ²	
Data / restraints / parameters	4987 / 210 / 354	
Goodness-of-fit on F ²	1.295	
Final R indices [I>2sigma(I)]	R1 = 0.0305, wR2 = 0.0889	
R indices (all data)	R1 = 0.0327, wR2 = 0.0987	
Extinction coefficient	n/a	
Largest diff. peak and hole	1.285 and -2.063 e.Å ⁻³	

Table S5. Atomic coordinates ($\times 10^4$) and equivalent isotropic displacement parameters ($\text{\AA}^2 \times 10^3$) for (PEA)₂PbI₄. U(eq) is defined as one third of the trace of the orthogonalized U^{ij} tensor.

	x	y	z	U(eq)
Pb(1)	5000	5000	5000	9(1)
Pb(2)	0	0	5000	9(1)
I(1)	5814(1)	5325(1)	6992(1)	20(1)
I(2)	3135(1)	1876(1)	5020(1)	12(1)
I(2A)	1872(7)	3124(7)	4983(4)	30(2)
I(3)	-670(1)	-180(1)	3010(1)	20(1)
I(4)	-1893(1)	3108(1)	5000(1)	12(1)
I(4A)	-3097(8)	1892(7)	5000(4)	32(2)
N(1)	9769(8)	6045(8)	6627(4)	25(1)
C(1)	10982(10)	5004(9)	6985(5)	24(2)
C(2)	10860(20)	4730(20)	7889(11)	28(3)
C(2A)	11730(20)	5590(20)	7905(11)	29(3)
C(3)	11160(20)	6230(20)	8441(10)	21(3)
C(3A)	10506(19)	5550(20)	8440(10)	20(3)
C(4)	12680(20)	6851(19)	8669(10)	24(3)
C(4A)	9958(19)	4170(20)	8654(10)	23(3)
C(5)	13000(20)	8240(20)	9168(11)	31(3)
C(5A)	8840(20)	4160(30)	9143(12)	37(4)
C(6)	11720(20)	9040(20)	9407(11)	35(3)
C(6A)	8180(20)	5490(30)	9400(11)	38(4)
C(7)	10240(20)	8440(20)	9167(10)	32(3)
C(7A)	8710(20)	6860(30)	9182(12)	39(4)
C(8)	9903(11)	6997(11)	8691(5)	32(2)
N(2)	6352(16)	1042(15)	6634(9)	20(3)
N(3)	4777(15)	-556(15)	6633(8)	19(3)
C(9)	5490(20)	-120(20)	7006(11)	26(4)
C(9A)	6100(20)	530(20)	7012(10)	23(3)
C(10)	6180(30)	-260(20)	7912(11)	25(3)
C(10A)	6720(20)	320(30)	7917(11)	25(3)
C(11)	6200(20)	1217(19)	8441(10)	20(3)
C(11A)	5480(18)	511(19)	8439(9)	16(2)
C(12)	7650(20)	2030(20)	8765(10)	26(3)
C(12A)	4876(19)	-790(20)	8768(10)	24(3)

C(13)	7620(30)	3440(20)	9242(11)	36(4)
C(13A)	3700(20)	-580(20)	9252(13)	38(4)
C(14)	6270(30)	4040(20)	9400(11)	39(4)
C(14A)	3160(20)	850(20)	9387(10)	34(4)
C(15)	4830(30)	3260(20)	9091(11)	34(4)
C(15A)	3690(20)	2150(20)	9072(10)	28(3)
C(16)	4869(10)	1896(10)	8622(5)	25(2)

Table S6. Experimental bond lengths (\AA) and angles ($^\circ$) of $(\text{PEA})_2\text{PbI}_4$.

Bond Length (\AA)		Bond Angle ($^\circ$)	
Pb(1)-I(2A)#1	3.150(6)	I(2A)#1-Pb(1)-I(2A)	180
Pb(1)-I(2A)	3.150(6)	I(2)#1-Pb(1)-I(2)	180
Pb(1)-I(2)#1	3.1536(5)	I(2)#1-Pb(1)-I(4)#2	89.290(13)
Pb(1)-I(2)	3.1536(5)	I(2)-Pb(1)-I(4)#2	90.710(13)
Pb(1)-I(4)#2	3.1747(5)	I(2)#1-Pb(1)-I(4)#3	90.710(13)
Pb(1)-I(4)#3	3.1748(5)	I(2)-Pb(1)-I(4)#3	89.290(13)
Pb(1)-I(4A)#2	3.181(7)	I(4)#2-Pb(1)-I(4)#3	180
Pb(1)-I(4A)#3	3.181(7)	I(2A)#1-Pb(1)-I(4A)#2	90.77(17)
Pb(1)-I(1)#1	3.2071(5)	I(2A)-Pb(1)-I(4A)#2	89.23(17)
Pb(1)-I(1)	3.2071(5)	I(2A)#1-Pb(1)-I(4A)#3	89.23(17)
Pb(2)-I(2)	3.1536(5)	I(2A)-Pb(1)-I(4A)#3	90.77(17)
Pb(2)-I(2)#4	3.1537(5)	I(4A)#2-Pb(1)-I(4A)#3	180
Pb(2)-I(2A)	3.156(6)	I(2A)#1-Pb(1)-I(1)#1	92.33(12)
Pb(2)-I(2A)#4	3.156(6)	I(2A)-Pb(1)-I(1)#1	87.67(12)
Pb(2)-I(4A)#4	3.167(7)	I(2)#1-Pb(1)-I(1)#1	90.682(13)
Pb(2)-I(4A)	3.167(7)	I(2)-Pb(1)-I(1)#1	89.318(13)
Pb(2)-I(4)	3.1758(5)	I(4)#2-Pb(1)-I(1)#1	88.562(13)
Pb(2)-I(4)#4	3.1759(5)	I(4)#3-Pb(1)-I(1)#1	91.438(13)
Pb(2)-I(3)	3.2046(5)	I(4A)#2-Pb(1)-I(1)#1	89.30(11)
Pb(2)-I(3)#4	3.2046(5)	I(4A)#3-Pb(1)-I(1)#1	90.70(11)
I(4)-Pb(1)#5	3.1748(5)	I(2A)#1-Pb(1)-I(1)	87.67(12)
I(4A)-Pb(1)#5	3.181(7)	I(2A)-Pb(1)-I(1)	92.33(12)
N(1)-C(1)	1.467(10)	I(2)#1-Pb(1)-I(1)	89.317(13)
N(1)-H(1A)	0.91	I(2)-Pb(1)-I(1)	90.682(13)
N(1)-H(1B)	0.91	I(4)#2-Pb(1)-I(1)	91.437(13)
N(1)-H(1C)	0.91	I(4)#3-Pb(1)-I(1)	88.563(13)
C(1)-C(2)	1.544(19)	I(4A)#2-Pb(1)-I(1)	90.70(11)
C(1)-C(2A)	1.57(2)	I(4A)#3-Pb(1)-I(1)	89.30(11)
C(1)-H(1BC)	0.99	I(1)#1-Pb(1)-I(1)	180.000(18)
C(1)-H(1BD)	0.99	I(2)-Pb(2)-I(2)#4	180
C(1)-H(1AA)	0.99	I(2A)-Pb(2)-I(2A)#4	180
C(1)-H(1AB)	0.99	I(2A)-Pb(2)-I(4A)#4	90.71(16)
C(2)-C(3)	1.52(2)	I(2A)#4-Pb(2)-I(4A)#4	89.29(16)
C(2)-H(2D)	0.99	I(2A)-Pb(2)-I(4A)	89.29(16)

C(2)-H(2E)	0.99	I(2A)#4-Pb(2)-I(4A)	90.71(16)
C(2A)-C(3A)	1.50(2)	I(4A)#4-Pb(2)-I(4A)	180
C(2A)-H(2AA)	0.99	I(2)-Pb(2)-I(4)	90.683(13)
C(2A)-H(2AB)	0.99	I(2)#4-Pb(2)-I(4)	89.317(13)
C(3)-C(8)	1.39(2)	I(2)-Pb(2)-I(4)#4	89.317(13)
C(3)-C(4)	1.40(2)	I(2)#4-Pb(2)-I(4)#4	90.683(13)
C(3A)-C(4A)	1.38(2)	I(4)-Pb(2)-I(4)#4	180
C(3A)-C(8)	1.428(19)	I(2)-Pb(2)-I(3)	89.360(13)
C(4)-C(5)	1.40(2)	I(2)#4-Pb(2)-I(3)	90.641(13)
C(4)-H(4)	0.95	I(2A)-Pb(2)-I(3)	87.71(12)
C(4A)-C(5A)	1.37(2)	I(2A)#4-Pb(2)-I(3)	92.29(12)
C(4A)-H(4A)	0.95	I(4A)#4-Pb(2)-I(3)	90.73(11)
C(5)-C(6)	1.41(3)	I(4A)-Pb(2)-I(3)	89.27(11)
C(5)-H(5)	0.95	I(4)-Pb(2)-I(3)	88.537(13)
C(5A)-C(6A)	1.36(3)	I(4)#4-Pb(2)-I(3)	91.463(13)
C(5A)-H(5A)	0.95	I(2)-Pb(2)-I(3)#4	90.640(13)
C(6)-C(7)	1.36(3)	I(2)#4-Pb(2)-I(3)#4	89.359(13)
C(6)-H(6)	0.95	I(2A)-Pb(2)-I(3)#4	92.29(12)
C(6A)-C(7A)	1.37(3)	I(2A)#4-Pb(2)-I(3)#4	87.71(12)
C(6A)-H(6A)	0.95	I(4A)#4-Pb(2)-I(3)#4	89.27(11)
C(7)-C(8)	1.42(2)	I(4A)-Pb(2)-I(3)#4	90.73(11)
C(7)-H(7)	0.95	I(4)-Pb(2)-I(3)#4	91.463(13)
C(7A)-C(8)	1.44(2)	I(4)#4-Pb(2)-I(3)#4	88.537(13)
C(7A)-H(7A)	0.95	I(3)-Pb(2)-I(3)#4	180
C(8)-H(8B)	0.95	Pb(1)-I(2)-Pb(2)	151.531(17)
C(8)-H(8A)	0.95	Pb(1)-I(2A)-Pb(2)	151.7(2)
N(2)-C(9)	1.48(2)	Pb(1)#5-I(4)-Pb(2)	152.949(17)
N(2)-H(2A)	0.91	Pb(2)-I(4A)-Pb(1)#5	153.2(2)
N(2)-H(2B)	0.91	C(1)-N(1)-H(1A)	109.5
N(2)-H(2C)	0.91	C(1)-N(1)-H(1B)	109.5
N(3)-C(9A)	1.49(2)	H(1A)-N(1)-H(1B)	109.5
N(3)-H(3A)	0.91	C(1)-N(1)-H(1C)	109.5
N(3)-H(3B)	0.91	H(1A)-N(1)-H(1C)	109.5
N(3)-H(3C)	0.91	H(1B)-N(1)-H(1C)	109.5
C(9)-C(10)	1.51(2)	N(1)-C(1)-C(2)	111.2(9)
C(9)-H(9A)	0.99	N(1)-C(1)-C(2A)	111.1(9)
C(9)-H(9B)	0.99	N(1)-C(1)-H(1BC)	109.4

C(9A)-C(10A)	1.51(2)	C(2A)-C(1)-H(1BC)	109.4
C(9A)-H(9AA)	0.99	N(1)-C(1)-H(1BD)	109.4
C(9A)-H(9AB)	0.99	C(2A)-C(1)-H(1BD)	109.4
C(10)-C(11)	1.49(2)	H(1BC)-C(1)-H(1BD)	108
C(10)-H(10A)	0.99	N(1)-C(1)-H(1AA)	109.4
C(10)-H(10B)	0.99	C(2)-C(1)-H(1AA)	109.4
C(10A)-C(11A)	1.50(2)	N(1)-C(1)-H(1AB)	109.4
C(10A)-H(10C)	0.99	C(2)-C(1)-H(1AB)	109.4
C(10A)-H(10D)	0.99	H(1AA)-C(1)-H(1AB)	108
C(11)-C(16)	1.375(19)	C(3)-C(2)-C(1)	110.5(13)
C(11)-C(12)	1.43(3)	C(3)-C(2)-H(2D)	109.5
C(11A)-C(16)	1.354(18)	C(1)-C(2)-H(2D)	109.5
C(11A)-C(12A)	1.42(2)	C(3)-C(2)-H(2E)	109.5
C(12)-C(13)	1.40(2)	C(1)-C(2)-H(2E)	109.5
C(12)-H(12)	0.95	H(2D)-C(2)-H(2E)	108.1
C(12A)-C(13A)	1.41(3)	C(3A)-C(2A)-C(1)	109.5(13)
C(12A)-H(12A)	0.95	C(3A)-C(2A)-H(2AA)	109.8
C(13)-C(14)	1.34(3)	C(1)-C(2A)-H(2AA)	109.8
C(13)-H(13)	0.95	C(3A)-C(2A)-H(2AB)	109.8
C(13A)-C(14A)	1.34(3)	C(1)-C(2A)-H(2AB)	109.8
C(13A)-H(13A)	0.95	H(2AA)-C(2A)-H(2AB)	108.2
C(14)-C(15)	1.41(3)	C(8)-C(3)-C(4)	120.7(15)
C(14)-H(14)	0.95	C(8)-C(3)-C(2)	119.4(15)
C(14A)-C(15A)	1.39(3)	C(4)-C(3)-C(2)	119.9(16)
C(14A)-H(14A)	0.95	C(4A)-C(3A)-C(8)	121.9(15)
C(15)-C(16)	1.368(19)	C(4A)-C(3A)-C(2A)	121.4(16)
C(15)-H(15)	0.95	C(8)-C(3A)-C(2A)	116.7(15)
C(15A)-C(16)	1.378(18)	C(3)-C(4)-C(5)	121.4(17)
C(15A)-H(15A)	0.95	C(3)-C(4)-H(4)	119.3
C(16)-H(16A)	0.95	C(5)-C(4)-H(4)	119.3
C(16)-H(16)	0.95	C(5A)-C(4A)-C(3A)	120.3(17)
		C(5A)-C(4A)-H(4A)	119.9
		C(3A)-C(4A)-H(4A)	119.9
		C(4)-C(5)-C(6)	118.0(18)
		C(4)-C(5)-H(5)	121
		C(6)-C(5)-H(5)	121
		C(6A)-C(5A)-C(4A)	121.6(19)

C(6A)-C(5A)-H(5A)	119.2
C(4A)-C(5A)-H(5A)	119.2
C(7)-C(6)-C(5)	120.2(18)
C(7)-C(6)-H(6)	119.9
C(5)-C(6)-H(6)	119.9
C(5A)-C(6A)-C(7A)	118.6(19)
C(5A)-C(6A)-H(6A)	120.7
C(7A)-C(6A)-H(6A)	120.7
C(6)-C(7)-C(8)	122.7(17)
C(6)-C(7)-H(7)	118.6
C(8)-C(7)-H(7)	118.6
C(6A)-C(7A)-C(8)	124.0(18)
C(6A)-C(7A)-H(7A)	118
C(8)-C(7A)-H(7A)	118
C(3)-C(8)-C(7)	116.9(14)
C(3A)-C(8)-C(7A)	113.7(14)
C(3A)-C(8)-H(8B)	123.2
C(7A)-C(8)-H(8B)	123.2
C(3)-C(8)-H(8A)	121.5
C(7)-C(8)-H(8A)	121.5
C(9)-N(2)-H(2A)	109.5
C(9)-N(2)-H(2B)	109.5
H(2A)-N(2)-H(2B)	109.5
C(9)-N(2)-H(2C)	109.5
H(2A)-N(2)-H(2C)	109.5
H(2B)-N(2)-H(2C)	109.5
C(9A)-N(3)-H(3A)	109.5
C(9A)-N(3)-H(3B)	109.5
H(3A)-N(3)-H(3B)	109.5
C(9A)-N(3)-H(3C)	109.5
H(3A)-N(3)-H(3C)	109.5
H(3B)-N(3)-H(3C)	109.5
N(2)-C(9)-C(10)	112.3(16)
N(2)-C(9)-H(9A)	109.2
C(10)-C(9)-H(9A)	109.2
N(2)-C(9)-H(9B)	109.2
C(10)-C(9)-H(9B)	109.2

H(9A)-C(9)-H(9B)	107.9
N(3)-C(9A)-C(10A)	113.1(16)
N(3)-C(9A)-H(9AA)	108.9
C(10A)-C(9A)-H(9AA)	108.9
N(3)-C(9A)-H(9AB)	108.9
C(10A)-C(9A)-H(9AB)	108.9
H(9AA)-C(9A)-H(9AB)	107.8
C(11)-C(10)-C(9)	113.6(15)
C(11)-C(10)-H(10A)	108.8
C(9)-C(10)-H(10A)	108.8
C(11)-C(10)-H(10B)	108.8
C(9)-C(10)-H(10B)	108.8
H(10A)-C(10)-H(10B)	107.7
C(11A)-C(10A)-C(9A)	112.2(14)
C(11A)-C(10A)-H(10C)	109.2
C(9A)-C(10A)-H(10C)	109.2
C(11A)-C(10A)-H(10D)	109.2
C(9A)-C(10A)-H(10D)	109.2
H(10C)-C(10A)-H(10D)	107.9
C(16)-C(11)-C(12)	116.4(14)
C(16)-C(11)-C(10)	123.1(16)
C(12)-C(11)-C(10)	120.4(16)
C(16)-C(11A)-C(12A)	116.5(14)
C(16)-C(11A)-C(10A)	123.0(15)
C(12A)-C(11A)-C(10A)	120.5(15)
C(13)-C(12)-C(11)	118.8(17)
C(13)-C(12)-H(12)	120.6
C(11)-C(12)-H(12)	120.6
C(13A)-C(12A)-C(11A)	119.4(16)
C(13A)-C(12A)-H(12A)	120.3
C(11A)-C(12A)-H(12A)	120.3
C(14)-C(13)-C(12)	122(2)
C(14)-C(13)-H(13)	119.1
C(12)-C(13)-H(13)	119.1
C(14A)-C(13A)-C(12A)	119.3(19)
C(14A)-C(13A)-H(13A)	120.4
C(12A)-C(13A)-H(13A)	120.4

C(13)-C(14)-C(15)	120.8(18)
C(13)-C(14)-H(14)	119.6
C(15)-C(14)-H(14)	119.6
C(13A)-C(14A)-C(15A)	123.8(18)
C(13A)-C(14A)-H(14A)	118.1
C(15A)-C(14A)-H(14A)	118.1
C(16)-C(15)-C(14)	116.9(17)
C(16)-C(15)-H(15)	121.5
C(14)-C(15)-H(15)	121.5
C(16)-C(15A)-C(14A)	114.8(16)
C(16)-C(15A)-H(15A)	122.6
C(14A)-C(15A)-H(15A)	122.6
C(15)-C(16)-C(11)	125.2(14)
C(11A)-C(16)-C(15A)	126.1(13)
C(11A)-C(16)-H(16A)	116.9
C(15A)-C(16)-H(16A)	116.9
C(15)-C(16)-H(16)	117.4
C(11)-C(16)-H(16)	117.4

Symmetry transformations used to generate equivalent atoms:

```
#1 -x+1,-y+1,-z+1 #2 -x,-y+1,-z+1 #3 x+1,y,z
#4 -x,-y,-z+1 #5 x-1,y,z
```

Table S7. Optical and static dielectric constants (ϵ_{∞} and ϵ_s), angular frequencies of a characteristic LO phonon mode (ω , in THz), average electron effective masses of bare electron bands (m^*), electron-phonon coupling constant (α) for $(EA)_2PbI_4$, $(AP)_2PbI_4$, $(PEA)_2PbI_4$, and tetragonal-phase $MAPbI_3$. The reported values of $MAPbBr_3$, $CsPbBr_3$ and $MAPbI_3$ calculated with the same method are given for comparison.

System	ϵ_{∞}	ϵ_s	ω (THz)	m^*	$\alpha_{\text{electron-phonon}}$
Tetragonal- $MAPbI_3$	4.73	33.42	4.11	0.200	2.299
$MAPbI_3$^a	4.5	24.1	2.25	0.12	2.39
$MAPbBr_3$^a	4.7	32.5	4.47	0.20	1.69
$MAPbBr_3$^b	4.4	21.4	5.81	0.13	1.54
$CsPbBr_3$^b	4.3	29.37	4.07	0.22	2.64
$(EA)_2PbI_4$	3.95	24.81	2.85	0.279	3.821
$(AP)_2PbI_4$	3.86	21.62	3.11	0.283	3.682
$(PEA)_2PbI_4$	3.38	20.85	3.38	0.307	4.285

- a. Frost, J. M. Calculating Polaron Mobility in Halide Perovskites. *Phys. Rev. B* **2017**, *96*, 195202
- b. Miyata, K.; Meggiolaro, D.; Trinh, M. T.; Joshi, P. P.; Mosconi, E.; Jones, S. C.; De Angelis, F.; Zhu, X. Y. Large Polarons in Lead Halide Perovskites. *Sci. Adv.* **2017**, *3*, e1701217.